



ELSEVIER

Journal of Alloys and Compounds 300–301 (2000) 389–394

Journal of  
ALLOYS  
AND COMPOUNDS

www.elsevier.com/locate/jallcom

## Optical transitions of $\text{Ho}^{3+}$ in YAG

M. Malinowski<sup>a,\*</sup>, Z. Frukacz<sup>a</sup>, M. Szuflińska<sup>a</sup>, A. Wnuk<sup>a,b</sup>, M. Kaczkan<sup>a</sup><sup>a</sup>Institute of Microelectronics and Optoelectronics PW, ul. Koszykowa 75, 00-662 Warsaw, Poland<sup>b</sup>Institute of Electronic Materials Technology, ul. Wólczyńska 133, 01-919 Warsaw, Poland

### Abstract

We report the optical properties of  $\text{Y}_3\text{Al}_5\text{O}_{12}$  (YAG) crystal doped with  $\text{Ho}^{3+}$  ions. Absorption, emission, and lifetime measurements have been performed and discussed using Judd–Ofelt theory. Visible emissions from the  $^3\text{D}_3$  (at about  $33\,000\text{ cm}^{-1}$ ),  $^5\text{S}_2$  ( $18\,500\text{ cm}^{-1}$ ) and  $^5\text{F}_5$  ( $15\,500\text{ cm}^{-1}$ ) excited states and IR emissions from the  $^5\text{I}_6$  level have been characterized under pulsed one-photon excitation and the experimental lifetimes for these levels have been compared with those obtained theoretically by using Judd–Ofelt approach. Upconversion processes for achieving blue and green fluorescence under one-color red and IR have been investigated. © 2000 Elsevier Science S.A. All rights reserved.

**Keywords:** Holmium; YAG– $\text{Ho}^{3+}$ ; Luminescence

### 1. Introduction

It is well known that  $\text{Ho}^{3+}$  ions can produce laser emission in the 2 and 2.9  $\mu\text{m}$  ranges [1–4] arising from transitions between Stark levels of the  $^5\text{I}_7$  and  $^5\text{I}_6$  states, respectively and the  $^5\text{I}_8$  ground state. As can be seen from the energy level diagram of trivalent holmium ( $\text{Ho}^{3+}$ ) [5], this ion has also several high lying metastable levels giving rise to transitions at various wavelengths from infrared (IR) to ultraviolet (UV) region. Crystals of  $\text{CaF}_2$  [6],  $\text{LiYF}_4$  [7] and  $\text{YAIO}_3$  [8] have been demonstrated to lase in the green part of the spectrum between transitions from the excited  $^5\text{S}_2$  state to the ground state [1,6]. The total number of reported laser channels of  $\text{Ho}^{3+}$  in insulating crystals is 14 (from 0.55 to 3.9  $\mu\text{m}$ ).

The first upconversion laser described by Johnson and Guggenheim in 1971 [9] was  $\text{BaY}_2\text{F}_8$  crystal doped by  $\text{Ho}^{3+} + \text{Yb}^{3+}$  ions and pumped by a filtered flash lamp. Allain et al. [10] demonstrated continuous wave (cw) green upconversion lasing in  $\text{Ho}^{3+}$  doped fluorozirconate glass fiber pumped by a red line of krypton laser. In 1994, Thrash et al. [11] reported cw upconversion green laser operation in  $\text{Yb}^{3+}$  codoped  $\text{KYF}_4$ – $\text{Ho}^{3+}$  crystals as the

result of  $\text{Yb}^{3+} \rightarrow \text{Ho}^{3+}$  energy transfer. Very recently, the  $\text{Ho}^{3+}$ –ZBLAN fiber upconversion laser has been examined in detail by Funk et al. [12,13].

These reported results stimulated our spectroscopic investigation of  $\text{Ho}^{3+}$  in various hosts for the purpose of establishing the properties that are important for laser action in the green region. Energy levels of  $\text{Y}_3\text{Al}_5\text{O}_{12}$  (YAG)– $\text{Ho}^{3+}$  were first studied in 1979 [14] but only recently they were determined in the wide energy range [15]. Polarized spectroscopy investigations of the dipole character of the holmium optical transitions in YAG were performed [16] and the measurements of upconversion energy transfer between  $\text{Ho}^{3+}$  ions in YAG excited in the IR region have been reported [17]. For holmium doped YAG [18] Judd–Ofelt [19,20] parameters, were calculated on a basis of limited number of transitions.

While emission properties of this system have been extensively studied in the near IR range, much less is known about the UV and visible emissions and their dynamics require more detailed investigation. The purpose of this work is to study the optical properties of  $\text{Ho}^{3+}$  in YAG crystal to better understand the behavior of rare-earth ion in this host and to predict its short wavelength emission properties. We performed optical absorption and emission transition intensity calculations, analyzed fluorescence dynamics and studied UV and visible luminescence properties of this material.

\*Corresponding author. Tel.: +48-22-660-7783; fax: +48-22-628-8740.

E-mail address: m.malinowski@imio.pw.edu.pl (M. Malinowski)

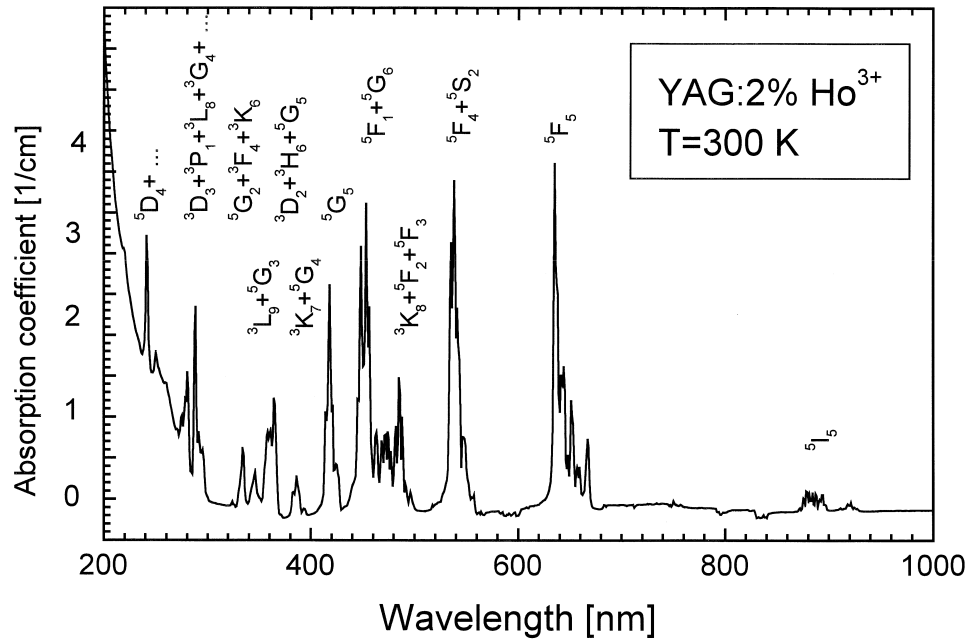


Fig. 1. Visible absorption spectrum of 2 at.%  $\text{Ho}^{3+}$ -YAG crystal at room temperature.

## 2. Results and discussion

### 2.1. Absorption and emission spectra

Single crystals of YAG doped by 0.1, 0.3, 2 and 5 at.% of  $\text{Ho}^{3+}$  were grown by the Czochralski method in the Institute of Electronic Materials Technology (ITME) in Warsaw. The experimental apparatus used to measure the sample absorption, luminescence and excitation spectra has

been described previously [21]. The room temperature absorption spectra in the 300–2300 nm range of 2%  $\text{Ho}^{3+}$  doped YAG are presented in Figs. 1 and 2. The figures show characteristic group of lines in the visible and near IR range, corresponding to  $4f^{10} \rightarrow 4f^{10}$  transitions of trivalent holmium ion. Below, at about 300 nm, the background absorption of the host crystal begins to increase and it grows rapidly at about 220 nm.

Emission of the crystals was recorded between 300 nm

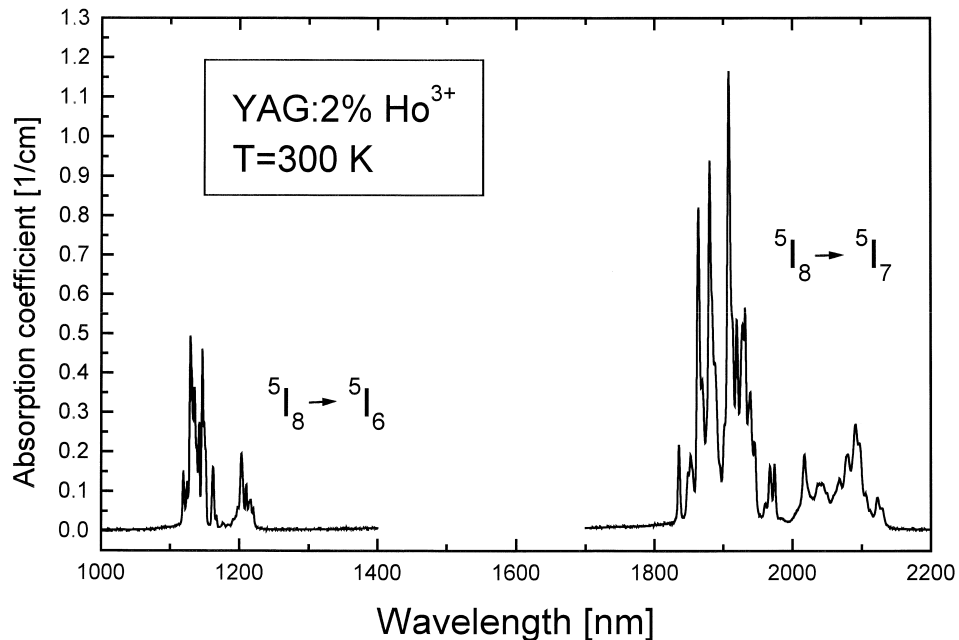


Fig. 2. Infrared absorption spectrum of 2 at.%  $\text{Ho}^{3+}$ -YAG crystal at room temperature.

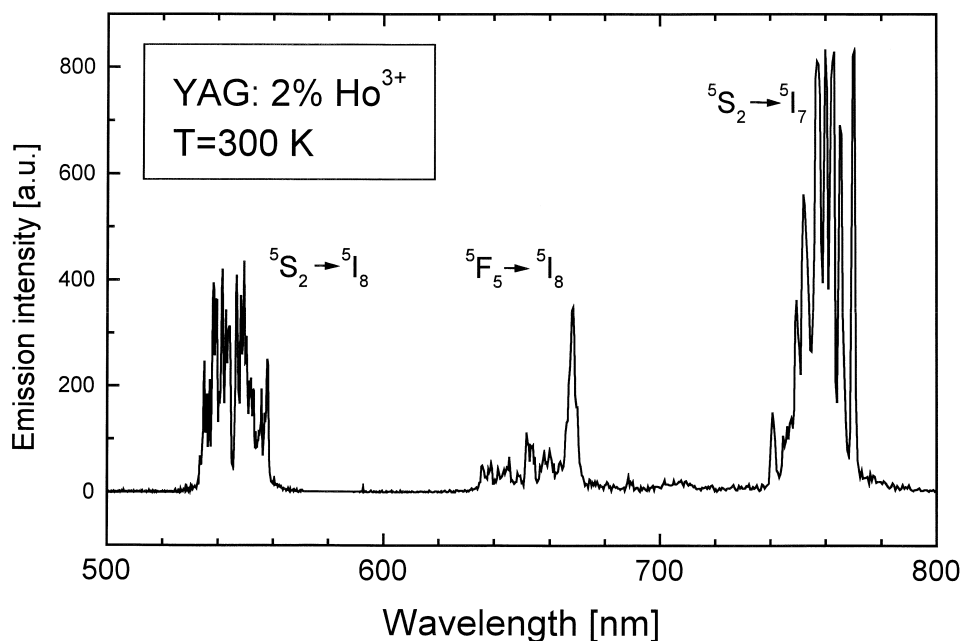


Fig. 3. Room temperature visible emission spectrum of  $\text{Ho}^{3+}$ -YAG crystal.

and 2  $\mu\text{m}$  after pulsed excitation at various wavelength. Fig. 3 illustrates the room temperature emission spectrum of 2%  $\text{Ho}^{3+}$ -YAG in the visible range, and in Fig. 4 IR part of the emission spectrum is shown in the same intensity scale. After UV and blue excitation, fluorescence is dominated by the transitions from the excited  $^3\text{D}_3$  state and  $^5\text{S}_2$  state, respectively. Weak emission originating from the  $^5\text{F}_5$  multiplet, populated by the non-radiative relaxation from the  $^5\text{S}_2$  could be observed in the 650 nm range. Near

IR spectrum consists of the emission band around 1  $\mu\text{m}$  resulting from the  $^5\text{I}_6 \rightarrow ^5\text{I}_8$  transitions. The experimentally observed emission transitions in YAG- $\text{Ho}^{3+}$  are summarized in Fig. 5.

## 2.2. Optical transition intensity analysis

Once the absorption spectrum has been measured, the Judd-Ofelt [19,20] intensity analysis was performed. Since

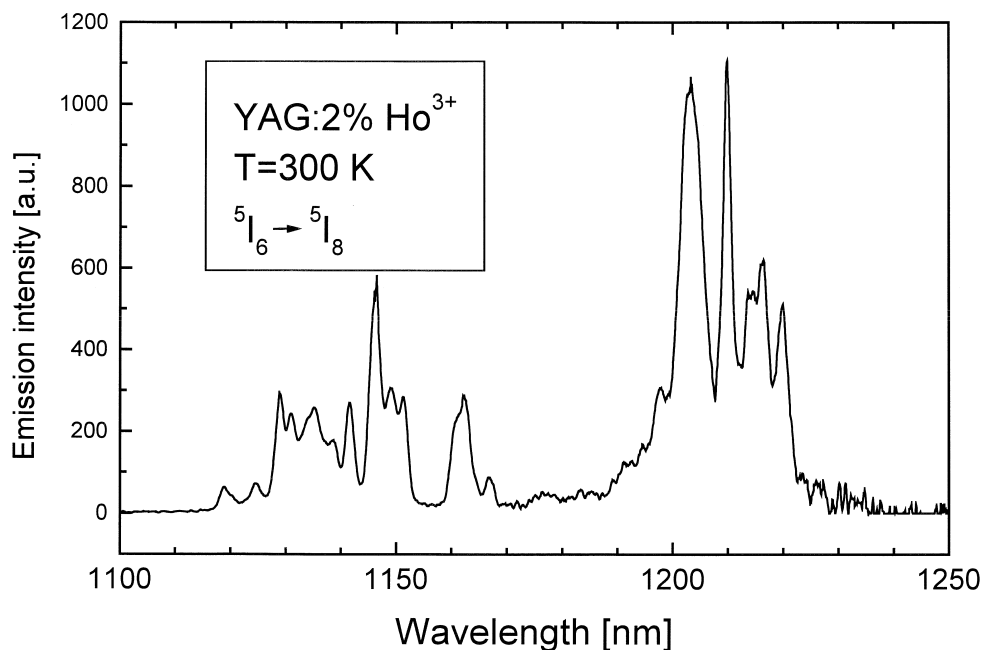


Fig. 4. Part of the IR emission spectrum of  $\text{Ho}^{3+}$ -YAG measured at 300 K.

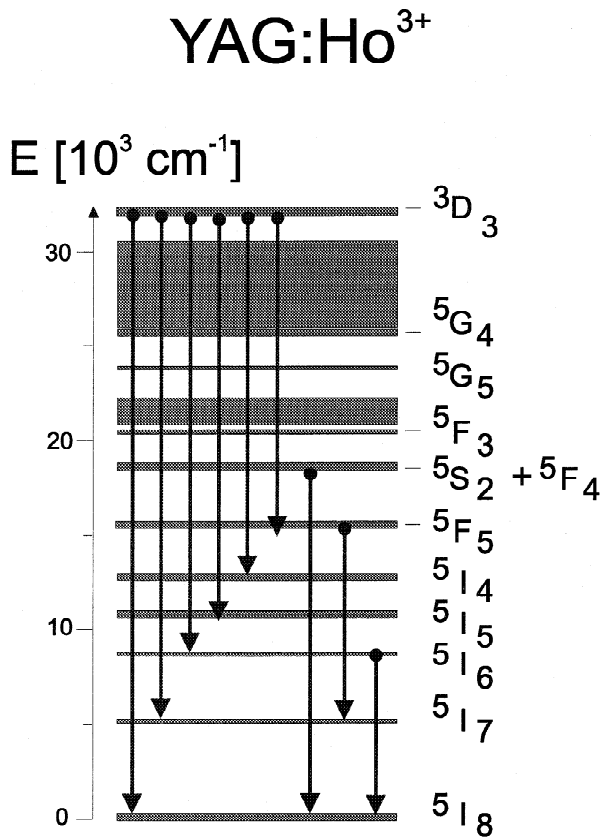


Fig. 5. Energy level scheme of Ho<sup>3+</sup> ion, observed emission transitions are indicated by arrows.

the details of the Judd–Ofelt theory, its precision and drawbacks have been extensively analyzed elsewhere [22] we have presented here only the essential results. The central result of the Judd–Ofelt theory is that the oscillator strength  $f_{\text{calc.}}$  of an electric dipole transition between rare-earth ion multiplets ( $J \rightarrow J'$ ) can be expressed by

$$f_{\text{calc.}}(aJ, bJ') = \frac{8\pi^2 m \nu}{3h(2J+1)n^2} \chi \sum_{t=2,4,6} \Omega_t |\langle 4f^n | a, J | U^{(t)} | 4f^n | b, J' \rangle|^2 \quad (1)$$

where  $h$  is Planck's constant,  $J$  is the angular momentum of the initial level,  $\chi = n(n^2 + 2)^2/9$  is a local field correction factor,  $\langle a || U^{(t)} || b \rangle$  are the doubly reduced matrix elements and  $\Omega_t$  are empirically determined parameters. The experimental oscillator strength  $f_{\text{exp}}$  for an absorption transition is defined as

$$f_{\text{exp}} = 4\pi\epsilon_0 \frac{mc^2}{N\pi e^2} \int \sigma(\nu) d\nu \quad (2)$$

where  $m$  and  $e$  are the electron mass and charge, respectively,  $c$  is the light velocity,  $\nu$  is the optical frequency and  $\sigma(\nu)$  is the absorption cross section.

From the least-square fit of measured ( $f_{\text{exp.}}$ ) and calculated ( $f_{\text{calc.}}$ ) oscillator strengths the three intensity  $\Omega_t$  parameters were evaluated. In performing the calculations the reduced matrix elements were taken from [23]. Table 1 shows the average wavelengths for the analyzed transitions together with the measured and calculated oscillator strengths for all the transitions observed in the absorption spectra. The resulting set of Judd–Ofelt parameters was found to be  $\Omega_2 = 0.04 \times 10^{-20} \text{ cm}^2$ ,  $\Omega_4 = 2.67 \times 10^{-20} \text{ cm}^2$  and  $\Omega_6 = 1.89 \times 10^{-20} \text{ cm}^2$ . A measure of the quality of the fit can be evaluated from the RMS deviation between the measured and calculated oscillator strengths values. The RMS deviation of  $8.9 \times 10^{-7}$  is comparable to values found by applying Judd–Ofelt theory to Ho<sup>3+</sup> ion in other systems [24]. However, Table 1 presents big difference between  $f_{\text{exp}}$  and  $f_{\text{calc.}}$  for  $^5I_8 \rightarrow ^5I_8$  transition which may be due to significant contribution of magnetic dipole mechanism. From the calculated set of  $\Omega_t$  intensity parameters the electric dipole transition probabilities  $A(aJ, bJ')$  for

Table 1  
Measured and calculated oscillator strengths for Ho<sup>3+</sup> ion in Y<sub>3</sub>Al<sub>5</sub>O<sub>12</sub><sup>a</sup>

[S'L'J'] manifold	$\lambda$ (nm)	$f_{\text{exp.}}$ ( $10^{-6}$ )	$f_{\text{calc.}}$ ( $10^{-6}$ )
<sup>5</sup> I <sub>7</sub>	1978	0.5868	1.7816
<sup>5</sup> I <sub>6</sub>	1169	0.3764	1.3194
<sup>5</sup> I <sub>5</sub>	899	0.2483	0.2480
<sup>5</sup> F <sub>5</sub>	651	3.8647	3.7441
<sup>5</sup> S <sub>2</sub> + <sup>5</sup> F <sub>4</sub>	546	4.7229	4.8878
<sup>5</sup> F <sub>3</sub> + <sup>5</sup> F <sub>2</sub> + <sup>3</sup> K <sub>8</sub>	481	4.0378	3.2629
<sup>5</sup> G <sub>6</sub> + <sup>5</sup> F <sub>1</sub>	454	5.8380	6.3437
<sup>3</sup> G <sub>5</sub>	421	3.6180	3.7411
<sup>5</sup> G <sub>4</sub> + <sup>3</sup> K <sub>7</sub>	388	0.7756	0.6675
<sup>5</sup> G <sub>5</sub> + <sup>3</sup> H <sub>6</sub> + <sup>3</sup> D <sub>2</sub>	364	4.6983	2.6986
<sup>5</sup> G <sub>3</sub> + <sup>3</sup> L <sub>9</sub>	347	0.4979	1.0899
<sup>3</sup> K <sub>6</sub> + <sup>3</sup> F <sub>4</sub> + <sup>5</sup> G <sub>2</sub>	335	0.6117	0.0392
<sup>3</sup> D <sub>3</sub> + ... + <sup>3</sup> I <sub>5</sub>	278	12.8560	14.8010

<sup>a</sup> RMS dev =  $8.9 \times 10^{-7}$ .

Table 2  
Calculated radiative transition probabilities, lifetimes and branching ratios for  $\text{Ho}^{3+}$  ion in YAG

Transition	$A_{ij}$ ( $\text{s}^{-1}$ )	$\tau_R$ (ms)	$\beta_{\text{calc.}}$
${}^5\text{F}_4 \rightarrow {}^5\text{S}_2$	$\approx 0.00$		$\approx 0.00$
$\rightarrow {}^5\text{F}_5$	5.22		0.00042
$\rightarrow {}^5\text{I}_4$	58.66		0.0047
$\rightarrow {}^5\text{I}_5$	376.37		0.0302
$\rightarrow {}^5\text{I}_6$	781.05		0.0627
$\rightarrow {}^5\text{I}_7$	1128.83		0.0907
$\rightarrow {}^5\text{I}_8$	10094.11	0.0804	0.8112
${}^5\text{S}_2 \rightarrow {}^5\text{F}_5$	0.72		0.00018
$\rightarrow {}^5\text{I}_4$	60.92		0.0156
$\rightarrow {}^5\text{I}_5$	58.57		0.0149
$\rightarrow {}^5\text{I}_6$	255.29		0.0653
$\rightarrow {}^5\text{I}_7$	1500.41		0.384
$\rightarrow {}^5\text{I}_8$	2036.18	0.256	0.521
${}^5\text{F}_5 \rightarrow {}^5\text{I}_4$	0.14		0.0000175
$\rightarrow {}^5\text{I}_5$	21.18		0.0026
$\rightarrow {}^5\text{I}_6$	307.33		0.0381
$\rightarrow {}^5\text{I}_7$	1450.51		0.1798
$\rightarrow {}^5\text{I}_8$	6285.29	0.124	0.7794
${}^5\text{I}_4 \rightarrow {}^5\text{I}_5$	11.31		0.0474
$\rightarrow {}^5\text{I}_6$	96.21		0.4029
$\rightarrow {}^5\text{I}_7$	124.88		0.5229
$\rightarrow {}^5\text{I}_8$	6.38	4.18	0.0267
${}^5\text{I}_5 \rightarrow {}^5\text{I}_6$	18.91		0.0349
$\rightarrow {}^5\text{I}_7$	304.72		0.5636
$\rightarrow {}^5\text{I}_8$	216.99	1.85	0.4014
${}^5\text{I}_6 \rightarrow {}^5\text{I}_7$	66.10		0.0899
$\rightarrow {}^5\text{I}_8$	668.93	1.36	0.91
${}^5\text{I}_7 \rightarrow {}^5\text{I}_8$	296.95	24.40	1.00

emission between  $J$  manifolds of  $\text{Ho}^{3+}$  were calculated using the equation

$$A(aJ, bJ') = \frac{64\pi^4 e^2 \nu^3}{3h(2J+1)c^3} \chi \sum_{t=2,4,6} \Omega_t |\langle 4f^n | a, J || U^{(t)} || 4f^n | b, J' \rangle|^2 \quad (3)$$

Calculated radiative transition probabilities  $A$  from the excited states together with the resulting branching ratios  $\beta_{\text{calc.}}$  are given in Table 2.

Radiative lifetimes of the  ${}^3\text{D}_3$ ,  ${}^5\text{S}_2$ ,  ${}^5\text{I}_6$  and  ${}^5\text{I}_7$  were calculated to be 131  $\mu\text{s}$ , 256  $\mu\text{s}$ , 1.36 ms, and 24 ms, respectively.

### 2.3. Fluorescence dynamics

Fig. 6 shows the decay profile of the  ${}^5\text{S}_2$  level measured at 15 K. The fluorescence lifetime was determined to be of 4.5  $\mu\text{s}$  which is, as could be seen from Table 3, much shorter than the radiative lifetime and the  ${}^5\text{S}_2$  lifetimes in other holmium activated materials, suggesting its predominantly nonradiative character. This is consistent with the small energy gap of  $2665 \text{ cm}^{-1}$  to the next lower lying level and high effective phonon energy in YAG.

The  ${}^3\text{D}_3$ , and  ${}^5\text{F}_5$  fluorescence decays in 0.1%  $\text{Ho}^{3+}$  doped YAG were found to be non-exponential, late time part of decays yields lifetimes of 2.7 and 0.3  $\mu\text{s}$ , respectively.

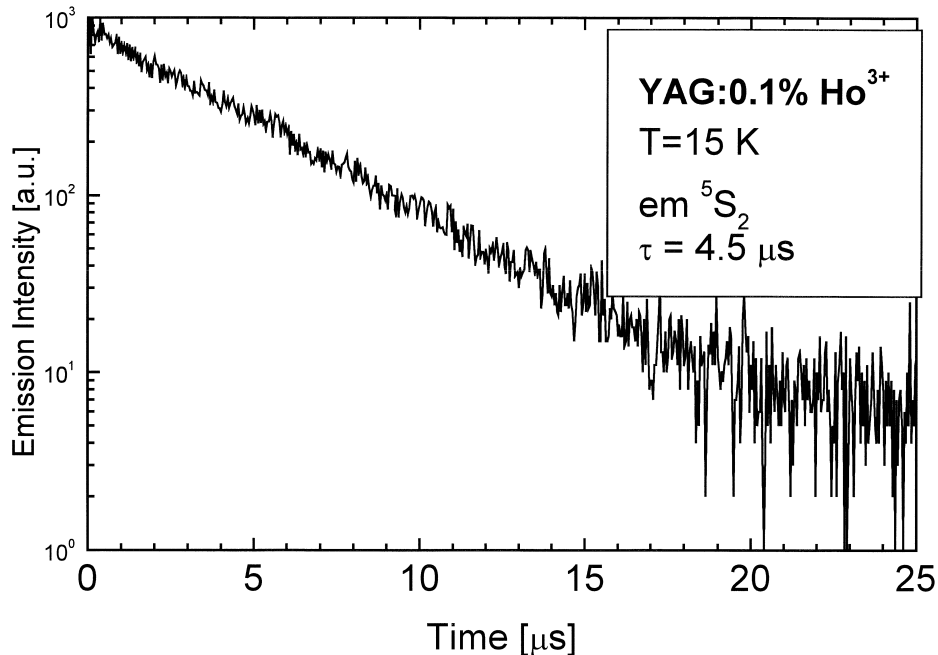


Fig. 6. Green fluorescence decay at 15 K in  $\text{Ho}^{3+}$ -YAG.

Table 3  
Comparison of the  $\text{Ho}^{3+}{}^5\text{S}_2$  lifetime measured in different materials

Material	${}^5\text{S}_2$ lifetime ( $\mu\text{s}$ )
$\text{Y}_3\text{Al}_5\text{O}_{12}$ -0.1% $\text{Ho}^{3+}$	4.5 [this work]
	4.7 [14]
$\text{Gd}_3\text{Ga}_5\text{O}_{12}$ - $\text{Ho}^{3+}$	63 [25]
ZBLAN glass	171 [24]
$\text{YAlO}_3$ -0.1% $\text{Ho}^{3+}$	83 [26]
$\text{LiYF}_4$ -0.2% $\text{Ho}^{3+}$	131.2 [27]
$\text{LaF}_3$ -0.5% $\text{Ho}^{3+}$	700 [28]
$\text{CaF}_2$ -1% $\text{Ho}^{3+}$	1030 [29]
$\text{LiNbO}_3$	14 [30]

### 3. Conclusions

The spectroscopic properties of  $\text{Ho}^{3+}$  ion in  $\text{Y}_3\text{Al}_5\text{O}_{12}$  crystals were studied and analyzed. Absorption spectra have been obtained leading to the determination of Judd–Ofelt intensity parameters and radiative transition probabilities. Because of the high effective phonon energy of the host matrix of about  $860\text{ cm}^{-1}$ , holmium ion fluorescence in YAG is strongly affected by nonradiative decay. Visible, green  $\text{Ho}^{3+}$  fluorescence presents much shorter lifetime to this of holmium in other oxide crystals.

### References

- [1] L.F. Johnson, H.G. Guggenheim, T.C. Rich, F.W. Ostermayer, J. Appl. Phys. 43 (1972) 1125.
- [2] D.W. Hart, M. Jani, N.P. Barnes, Optics Lett. 21 (1996) 728.
- [3] A.A. Kaminskii, T.I. Butaeva, A.O. Ivanov, T.V. Mochalov, A.G. Petrosyan, G.I. Rogov, V.A. Fedorov, Sov. Tech. Phys. Lett. 2 (1976) 308.
- [4] A.A. Kaminskii, V.A. Fedorov, S.E. Sarkisov, J. Bohm, P. Reiche, D. Scultze, Ohys. Stat. Solidi (a) 53 (1979) K219.
- [5] G.H. Dieke, H.M. Crosswhite, Appl. Opt. 2 (1963) 675.
- [6] Yu.K. Voronko, A.A. Kaminskii, V.V. Osiko, A.M. Prokhorov, JETP Lett. 1 (1965) 3.
- [7] I.G. Podkolzina, A.M. Tkaczuk, V.A. Fedorov, P.P. Feofilov, Opt. Spektroskopiya 40 (1976) 196.
- [8] A.A. Kaminskii, V.M. Garmosh, G.A. Ermakov, V.A. Akkerman, A.A. Filmonov, K. Kurbarov, Izv. Akad. Nauk SSSR, Ser. Neorg. Mater. 22 (1986) 1576.
- [9] L.F. Johnson, H. Guggenheim, Appl. Phys. Lett. 19 (1971) 44.
- [10] J.Y. Allain, M. Monerie, H. Poignant, Electron. Lett. 26 (1990) 261.
- [11] R.J. Thrash, R.H. Jarman, B.H.T. Chai, A. Pham, in: Topical Meeting on Compact Blue-Green Lasers, February 10–14, 1994, Salt Lake City, CFA5-1/73, 1994.
- [12] D.S. Funk, J.G. Eden, IEEE J. Sel. Top. Q.E. 1 (1995) 784.
- [13] D.S. Funk, S.B. Stevens, S.S. Wu, J.G. Eden, IEEE J.Q.E. 32 (1996) 638.
- [14] M.K. Ashurov, Yu.K. Voronko, E.W. Zarikov, A.A. Kaminskii, V.V. Osiko, A.A. Sobol, M.I. Timoshechkin, W.A. Fedorov, A.A. Szabaltai, Neorg. Mat. 15 (1979) 1250.
- [15] J.B. Gruber, M.J. Hills, M.D. Seltzer, S.B. Stevens, C.A. Morrison, G.A. Turner, M.R. Kokta, J. Appl. Phys. 69 (1991) 8183.
- [16] M.D. Selzer, M.E. Hills, J.B. Gruber, Phys. Rev. B 46 (1992) 8007.
- [17] L.B. Shaw, R.S. Chang, N. Djeu, Phys. Rev. B 50 (1994) 6609.
- [18] B.M. Antipienko, Yu.W. Tomaszewicz, Optik. Spektrosk. 44 (1978) 272.
- [19] B.R. Judd, Phys. Rev. 127 (1962) 750.
- [20] G.S. Ofelt, J. Chem. Phys. 37 (1962) 511.
- [21] M. Malinowski, R. Piramidowicz, J. Sarnecki, W. Woliński, J. Phys.: Condens. Matter 10 (1998) 1909.
- [22] A.A. Kaminskii, Crystalline Lasers, CRC Press, 1996.
- [23] W.T. Carnall, H. Crosswhite, H.M. Crosswhite, Energy Level Structure and Transition Probabilities of the Trivalent Lanthanides in  $\text{LaF}_3$ , Argonne National Laboratory, Argonne, IL, 1975.
- [24] K. Tanimura, M.D. Shinn, W.A. Sibley, M.G. Drexhage, R.N. Brown, Phys. Rev. B 30 (1984) 2429.
- [25] A. Brenier, L.C. Courrol, C. Pedrini, C. Madej, G. Boulon, Opt. Mater. 3 (1994) 25.
- [26] M. Malinowski, R. Piramidowicz, Z. Frukacz, G. Chadeyron, R. Mahiou, M.F. Joubert, Optical Mater. 12 (1999) 409.
- [27] L. Gomes, L.C. Corrol, L.V.G. Tarelho, I.M. Ranieri, Phys. Rev. B 54 (1996) 3825.
- [28] B.R. Reddy, S. Nash-Stevenson, P. Venkateswarlu, J. Opt. Soc. Am. B 11 (1994) 923.
- [29] S.R. Bullock, B.R. Reddy, P. Venkateswarlu, S. Nash-Stevenson, J. Opt. Soc. Am. B 14 (1997) 553.
- [30] A. Lorenzo, L.E. Baussa, J.A. Sanz Garcia, J. Garcia Sole, J. Phys.: Condens Matter 8 (1996) 5781.